Journal of Engineering Mathematics **28**: 43–54, 1994.

On the simultaneous measurements of two velocity components in the turbulent spot

A. SEIFERT, M. ZILBERMAN and I. WYGNANSKI

Department of Fluid Mechanics and Heat Transfer, Faculty of Engineering, Tel Aviv University, Ramat-Aviv, Israel 66978

Received 1 December 1992; accepted in revised form 13 September 1993

Abstract. Measurements of spanwise and streamwise velocity components in a turbulent spot artificially initiated in a Blasius boundary layer are described. A special hot-wire rake consisting of 8 'V' shaped arrays was built for this purpose. This multi-probe rake also enabled one to align the individual realizations in both streamwise and spanwise directions and to form more representative ensemble-averages near the tip of the spot. The data reveals the existence of a strong spanwise component of velocity which attains its maximum value at the tip of the spot and is centered around an elevation equivalent to the displacement thickness of the unperturbed boundary layer. This perturbation velocity resembles a wave which follows the leading interface of the spot and may therefore be amenable to analysis.

Introduction

There is abundance of evidence suggesting that the interior structure of a transitional spot embedded in a Blasius boundary layer is similar to a fully developed turbulent boundary layer. Thus, the manner in which the turbulent spot destabilizes the surrounding vortical fluid is of interest to those attempting to delay transition as well as those interested in the structure and control of the turbulent boundary layer. The spot spreads in the spanwise and streamwise directions at an incredible rate in the absence of favourable streamwise pressure gradient. Since the fluid within the laminar boundary layer surrounding the spot is already vortical, the propagation of the spot-interface near the solid surface may be achieved by destabilizing the flow surrounding the spot. The destabilization process is enhanced when the surrounding boundary layer is unstable to small disturbances of the Tollmien–Schlichting type. In this case two, oblique wave packets, trailing the spot amplify and break down to generate new turbulent spots which soon coalesce with the 'parent' spot [1, 2]. Such wave packets are absent when the surrounding boundary layer is stable [3] and their absence is associated with diminishing the rate of spread of the spot in the direction of streaming. The absence of breakdown to turbulence near the trailing interface of the spot affects the shape of the trailing interface changing the plan-view of the spot from its typical 'arrow head' (or heart-like) shape to a triangular shape with the trailing interface perpendicular to the direction of streaming. However, despite the stable surroundings, the spot keeps spreading in a manner which is only vaguely understood.

In an attempt to correlate the internal structure of the spot with its rate of spread and formulate the latter within the context of the classical stability theory it was decided to measure carefully the lateral component of velocity associated with the passage of the spot in otherwise a laminar boundary layer. A special hot-wire rake was built for this purpose and the principal results of the investigation are reported in this manuscript.

Some novel experimental procedures

The free stream velocity in the present experiment was maintained at 11.4 m/sec throughout and the measurements were made at $6.65*10^5 \leq Re_x \leq 10.2*10^5$ based on the distance measured from the leading edge of the plate. The spot was initiated artificially by a spark located at $X = 30$ cm and $Z = 0$.

Since the experimental apparatus, data acquisition and some of the reduction techniques are described in earlier papers [4, 2] the reader is directed to those sources for additional information. Very detailed measurements were made near the tip of the spot (i.e. at 80 mm $\leq Z \leq$ 96 mm) at the first measuring station ($X = 90$ cm, $X_s = 60$ cm). This data was acquired at 10 elevations from the plate varying between $0.5 < Y/\delta^*_{laminar} < 3$. Special attention was paid to the regions in which the velocity gradients were high.

A photograph of the 16-wire 'V' probe used in this experiment is shown in Fig. 1. The Z resolution of each V array is approximately 1.7 mm and the average distance between adjacent centers of the V arrays is 2.3 mm. Consequently, simultaneous two-component velocity data is provided by this rake over an aggregate span of 16.04 mm corresponding to the distance between the centers of the first and the last V array in the rake. The rake was mounted on a traversing mechanism having 6 degrees of freedom corresponding to translation in the X, Y, Z directions and rotation around all three axes. Translation in the Y direction and rotation around the Y axis were computer controlled because the rake had to be moved out of the boundary layer to be calibrated in yaw. The maximum resolution provided by the stepper motor was 12.7 μm in Y and 0.3° in yaw. Manual rotation around the X and Z axes enabled one to align the rake parallel to the plate and normal to the direction of streaming.

Yaw and speed calibration was made by using 'look-up' tables of 4096 (corresponding to the 12 bit resolution of the analog-to-digital converter) points per wire. The experiment was conducted at a free stream velocity of $U_\infty = 11.4$ m/s and therefore the velocity calibration carried out between 1.5 m/s and 12 m/s. This range was subdivided into 7 segments and a fourth order polynomial was fitted to the data. The accuracy of the velocity calibration in the direction of streaming was within 1% of U_∞. Since the hot-wires in each V array were inclined to the rake axis by 45°, yaw calibration was restricted to ±33° only and was done at

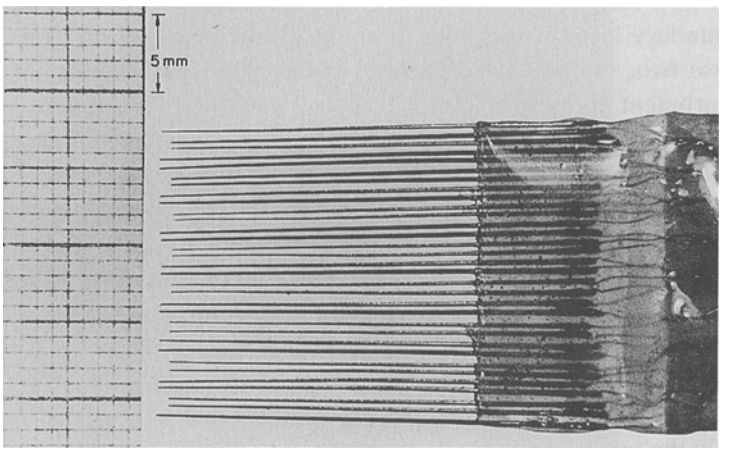

Fig. 1. A picture of the hot wire rake.

6° interval. The restriction on the yaw angle provided a limitation on the minimum distance from the surface at which measurements could be done. The streamwise and spanwise velocity components were obtained from a pair of voltages recorded simultaneously by each wire (E_1 and E_2) in the 'V' array (Fig. 2). Classical spline and interpolation techniques were used to generate a 'look-up' table correlating the instantaneous two-dimensional velocity vector to the E_1 and E_2 voltages. It was required that the measured voltages were within the calibration range during the passage of the spot. The hot-wire calibration was tested for drift and if found acceptable the rake was moved to the measuring station in the boundary layer. Final alignment of the rake was done in laminar flow where the local velocity was $0.3U_\infty$. Two conditions were imposed on each V-array at this location:

(i) that the velocity gradient around this location was linear and the extrapolated distance to the wall measured by all the arrays was approximately equal.

(ii) that the spanwise component of velocity measured by each array was sufficiently small so that the inclination angle measured did not exceed 2°.

All these requirements could be met, under normal operating conditions, provided the nominal distance of the rake from the wall was 1 mm or larger. The sampling frequency was 4 KHz per channel and the number of events recorded at each measuring station varied between 400 and 600. The larger number of events was recorded near the wall where the probability to encounter events outside the calibration range was higher (Fig. 2). Data processing was too slow to make the transformation from voltage to velocity in real time, thus, whenever the calibration range was exceeded during the 'off-line' processing of the data that entire event was discarded reducing the pool of the available events for ensemble-averaging. Whenever the rake elevation was reduced below 1 mm, in the range of X locations considered, 30%–50% of the events were lost in this manner.

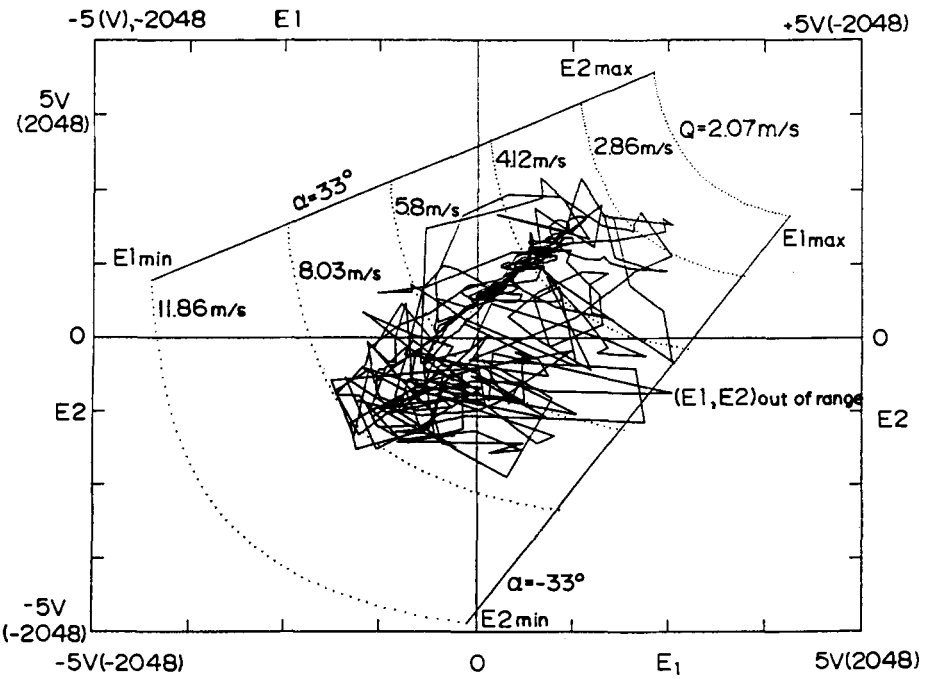

Fig. 2. Calibration test of the 'V' shaped probe in the wall region during the passage of a turbulent spot.

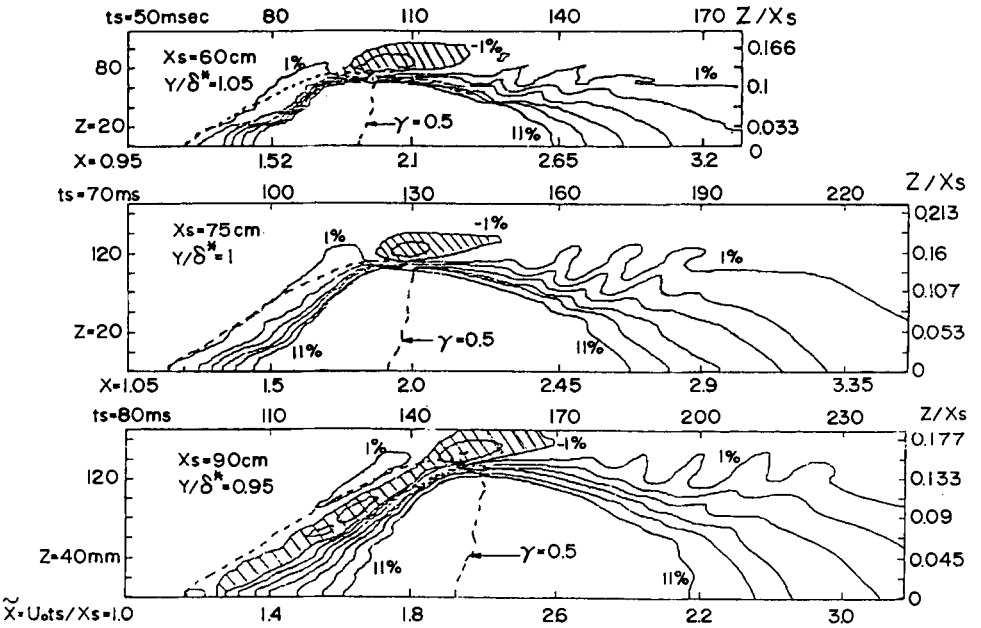

Fig. 3. Ensemble averaged streamwise velocity perturbations observed during the passage of the spot.

Discussion of results

Ensemble averaged, streamwise velocity perturbation contours recorded during the passage of the spot are plotted in Fig. 3. These data were plotted in the (Z, T) plane at an approximate elevation above the surface which is equivalent to the displacement thickness of the unperturbed, laminar boundary layer (i.e. at $\delta^* \simeq 1$). The measurements presented were made at 3 streamwise locations: 60, 75, and 90 cm downstream of the spark generator or 90, 105, and 120 cm downstream of the leading edge of the plate. The perturbation contour levels observed vary from -3% to $+11\%$ and are plotted at intervals of 2%. The negative velocity perturbation regions are hatched. The dimensional spanwise distance is marked on the left of each figure while the time elapsed from the initiation of the spot by the spark is marked on top. The corresponding dimensionless streamwise ($\tilde{X} = U_0 t_s / X_s$; where the subscript '$s$' refers to times and distances measured from the origin of the spot and U_0 is the free stream velocity) and spanwise (Z/X_s) distances are marked at the bottom and right side of each figure. The average location of the interface determined by the intermittency factor [2] $\gamma = 0.5$ is also marked in Figs. 3 and 4 by a dashed line.

There is a steep positive gradient in the steamwise velocity component (Fig. 3) following the leading edge of the spot at the first two streamwise locations (i.e. at $X_s = 60$ and 75 cm). There is a region of negative velocity perturbation beyond the tip of the spot (i.e. at $Z/X_s > 0.15$ and $X = 2$) at all streamwise locations measured. At $X_s = 90$ cm the negative velocity perturbation extends from the tip of the spot to its plane of symmetry (i.e. to $Z = 0$). The continuous region of negative velocity perturbation under the 'overhang' of the leading interface was never shown although it could have been inferred from the data presented in Ref. [4]. Closer to the solid surface there is only a positive velocity perturbation [2]. It suggests that the initial breakdown to turbulence is associated with an ejection of low velocity fluid from the surface outward (see Fig. 11a of Ref. [7]) before the effective

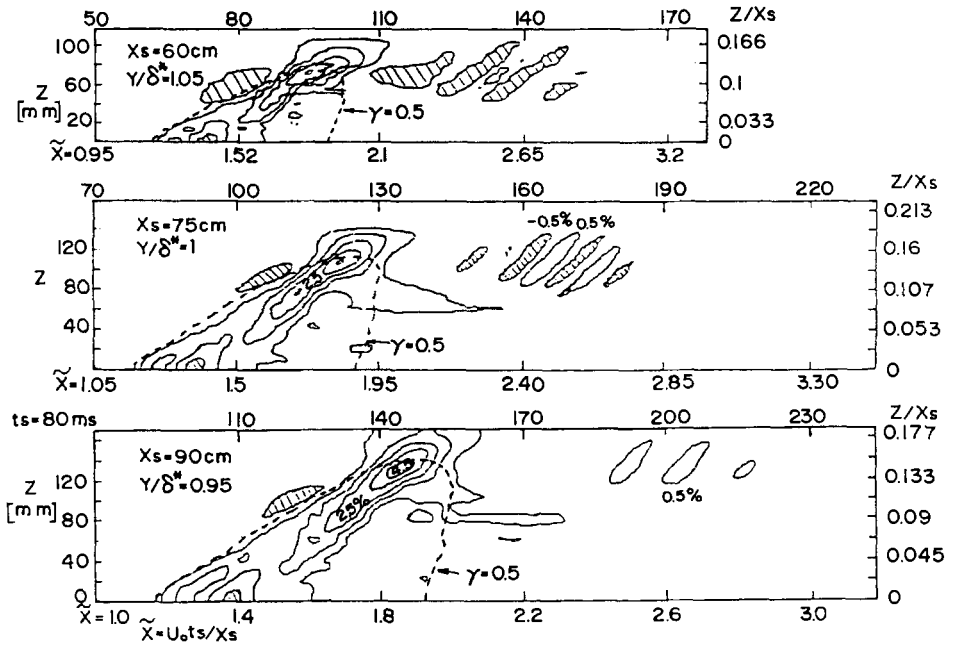

Fig. 4. Ensemble averaged spanwise velocity perturbations observed during the passage of the spot.

turbulent mixing enhances the velocity near the surface. It is quite possible that the reason for not seeing this at smaller X_s distances stems from the short duration of the event relative to the jitter in the time of arrival of the spot but it may also be a phenomenon which evolves whenever the spot attains some form of equilibrium. The negative velocity perturbation region follows the leading interface so precisely that the two occurrences are probably interconnected.

The high velocity region following the spot, or the 'calmed' region in the parlance of Schubauer and Klebanoff [5], exceeds in length the turbulent length of the spot at all Z locations. The wave packets following the spot are also observed at all three streamwise locations shown. The number of wave-crests in the packet increases with X_s, while the distance separating the first wave-crest from the trailing interface of the spot did not change between $X_s = 60$ cm and $X_s = 90$ cm. The ensemble averaged amplitudes of the waves have diminished at $X_s = 90$ cm because of partial breakdown to turbulence and possibly due to enhanced jitter before breakdown. In fact a 20% intermittency factor contour was measured between $2.2 < (U_\infty T/X_s) < 2.6$ centered around $Z/X_s = 0.08$. These results are in agreement with the data presented in Ref. [2] at $Y/\delta^* \simeq 0.6$.

The corresponding W-perturbation contours are plotted in Fig. 4 for the identical locations discussed above. The contour levels plotted vary between -0.5% and $+4.5\%$ at intervals of 1% where the positive sign implies outward direction from the plane of symmetry. It is interesting to note that the maximum outward (positive) velocity measured at $Y/\delta^* \simeq 1$ is located inside the turbulent zone near the leading interface at the tip of the spot. The contours of the cross-flow component follow the leading interface of the spot and are entirely absent from its core, its trailing edge and from the 'calmed-flow' regions. The inflow (i.e. negative W) contours outside the turbulent zone coincide with an excess of the streamwise velocity outside the spot boundaries. This is seen most clearly in the wave packet region and

just prior to the arrival of the spot and suggests that there might be also a wave activity near the leading interface. Both W and dW/dZ essentially vanish near the plane of symmetry [4].

Conditionally aligned perturbation contours in the Y-T plane measured near the tip of the spot (i.e. $0.137 \leq Z/X_s \leq 0.160$) are shown in Figs. 5 and 6. The velocity perturbations recorded by the rake during the passage of the spot enabled one to detect the instantaneous

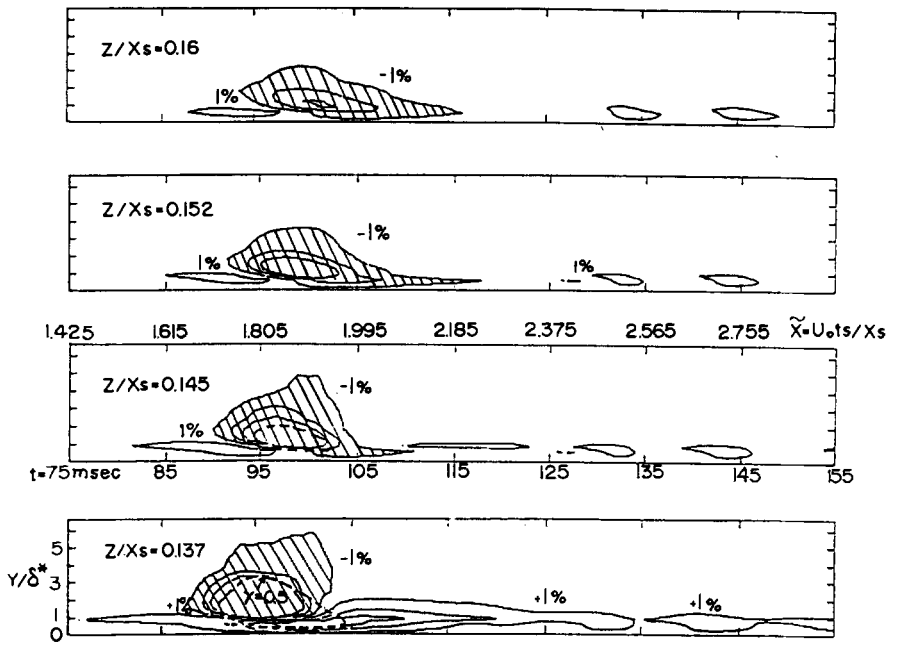

Fig. 5. Ensemble averaged streamwise velocity perturbations in the Y-t plane near the tip of the spot, $X_s = 60$ cm.

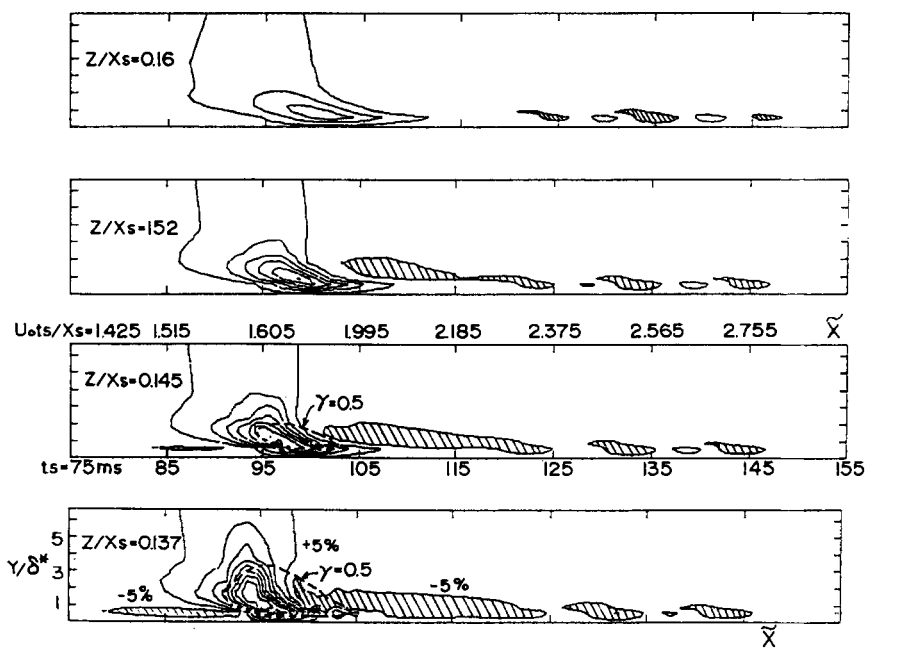

Fig. 6. Ensemble averaged streamwise velocity perturbations in the Y-t plane near the tip of the spot, $X_s = 60$ cm.

location of the turbulent interface for each event. The rake was positioned in such a way that the average location of the spot tip occurred at its center. The data was then shifted in the Z direction in order to represent the flow relative to the average location of the interface. The maximum, ensemble averaged cross-flow velocity was increased in this manner from $0.045U_\infty$ (shown in Fig. 4) to $0.08U_\infty$ (Fig. 6). Some individual realizations indicated that the maximum spanwise velocity W could be as high as $0.17U_\infty$ implying that the alignment of the data can still be improved. This is important because the spanwise rate of spread of the spot would become comparable to the average inclination of the velocity vector measured at the tip of the spot to the plane of symmetry.

The excess in the streamwise velocity perturbation near the wall, so prominent in the vicinity of the plane of symmetry [6, 7] totally disappears from within the turbulent region at $Z/X_s \geq 0.145$ (Fig. 5). Only some wavy remnants of the 'calmed region' are observed at this span-wise location, however, the excess velocity under the 'overhang' of the leading interface persists to the very tip of the spot (Fig. 5). The perturbed low speed fluid appears to be transported away from the plane of symmetry by the outward perturbation in W (Fig. 6). The maximum cross-flow velocity educed is approximately 8% of U_∞ at $Z/X_s \simeq 0.13$ and it reduces to 6.5% near the average location of the tip. It was postulated before (Ref. [2], Fig. 14) that the waves in the packet might turn in the streamwise direction and coalesce distorting the mean velocity behind the spot and generating the 'calmed region'. The relatively prominent transverse velocity in the inflow direction following the spot (observed in Fig. 6 at: $0.137 < Z/X < 0.160$) tend to reinforce this notion.

The ensemble averaged velocity perturbation normal to the surface can be calculated from the rake data by using continuity and assuming that the spot is propagating in the direction of streaming at $0.65U_\infty$. Although it is not claimed to be an accurate technique it provides some insight into the structure of the flow. Thus all three components of perturbation velocity corresponding to $Z/X_s = 0.137$ are presented in Fig. 7. A strong upwash (V positive) velocity perturbation equivalent to $3.5\%U_\infty$ is visible above the leading interface of the spot. The strongest upwash does not coincide with the strongest cross flow or streamwise velocity

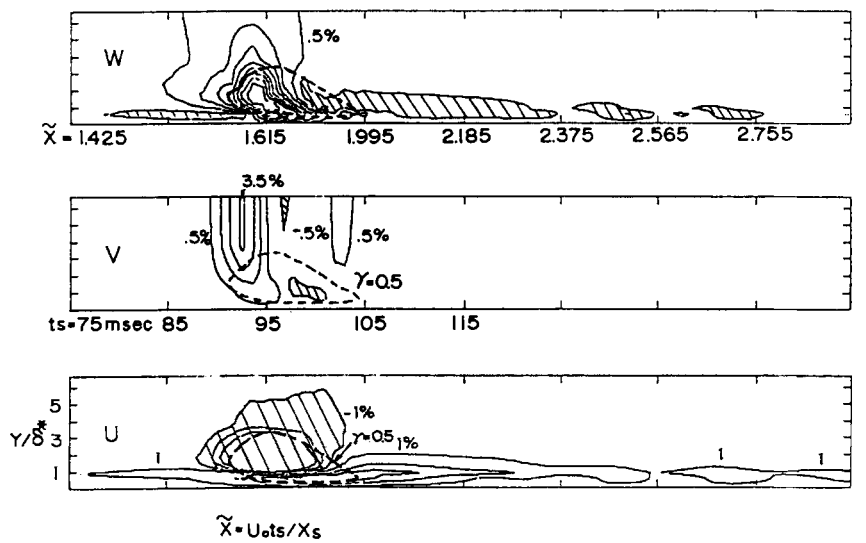

Fig. 7. The three components of the ensemble averaged velocity perturbation measured at $X_s = 60$ cm and $Z/X_s = 0.137$.

perturbations, it is also confined to the streamwise extent of the spot while the inwash (the negative W perturbation) and the streamwise velocity perturbations linger for a long time behind the trailing interface at this Z cross section.

Plotting vector diagrams in the Y-t plane (Fig. 8) and in the Z-t plane (Fig. 9) near the

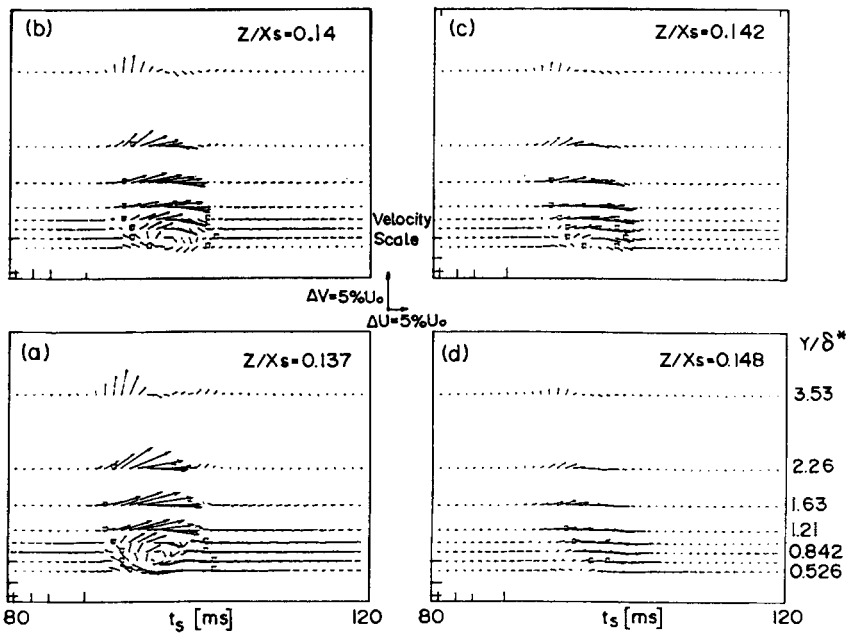

Fig. 8. Vector diagrams of the perturbation velocities in the Y-t plane near the tip of the spot, $X_s = 60$ cm.

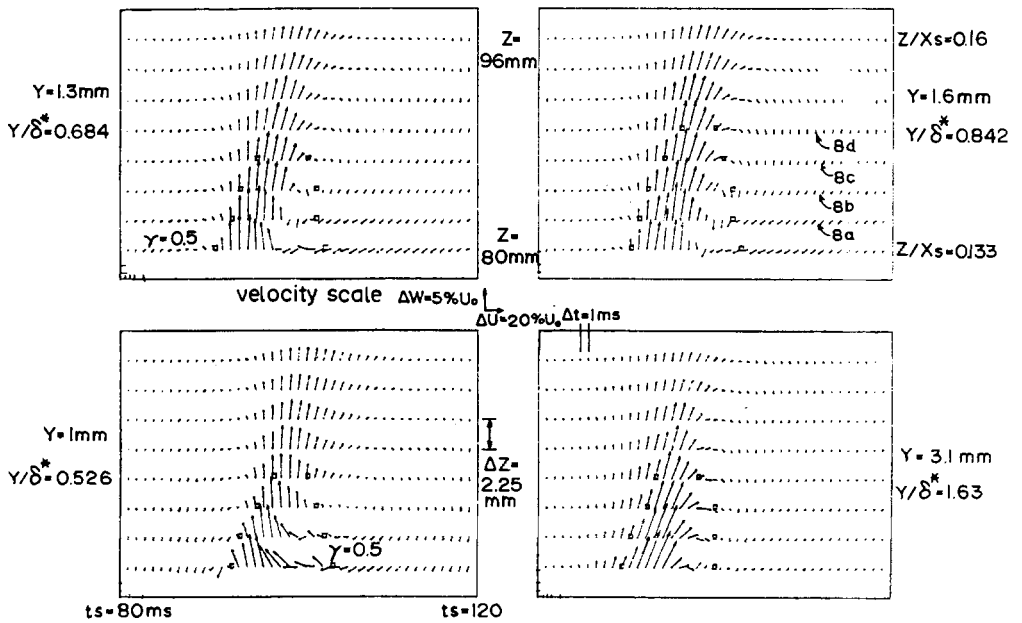

Fig. 9. Vector diagrams of the perturbation velocities in the Z-t plane near the tip of the spot, $X_s = 60$ cm (the cross sections plotted in Fig. 8 are marked in the top right figure).

outer tip of the spot indicates that the velocity perturbations associated with the passage of the tip of the spot can be represented by coherent vortices. The core of the spanwise vortex is situated below $Y/\delta^* = 1$ and inboard of $Z/X_s = 0.140$ (Fig. 8) while at larger Z the spanwise vorticity perturbation occurs near the surface. The center of the vertical vortex (Fig. 9) is located near the trailing interface of the tip (the location of the mean position of the interface is marked by square symbols in Figs. 8 and 9) and its effects are felt beyond $Z/X_s = 0.160$. Although velocity vectors give only a qualitative representation of circulation there can be little doubt about the presence of strong perturbation vorticity in this region. These observations are consistent with the presence of single arm of the classical 'horse-shoe' or 'Λ' shaped vortex situated near the tip of the spot which is sufficiently coherent to be detected in spite of the averaging process. An intensive search for the second arm of the 'horse-shoe' did not yield positive results to date.

Examining the vector diagrams in the Z-t plane over the entire span of the spot at $Y/\delta^* \simeq 1$ and $X_s = 75$ cm gives no indication that other 'Λ' vortices exist. The averaged data suggest that a single vortex spanning the spot parallel to its leading edge dominates the transition process. One may even notice a periodicity in the pattern between $0 < Z/X_s < 0.06$ (Fig. 10). The period is approximately 13 msec and it corresponds to the dominant period of the Tollmien–Schlichting wave-packet which trails the spot. One may surmise from this information that the breakdown to turbulence occurs along the leading edge of the spot and it may be associated with an instability mechanism.

A contour plot of the turbulent intensity (a 'true RMS' defined in Ref. [2]) is shown in Fig. 11 for the data presented in Figs. 3 and 4 at $X_s = 90$ cm. These contours indicate that most of the turbulent activity below the 'overhang' of the leading interface is associated with the above-mentioned vortex or wave. The intensity gradients near the boundaries can be enhanced by accounting for the intermittency factor of the average time of arrival of the

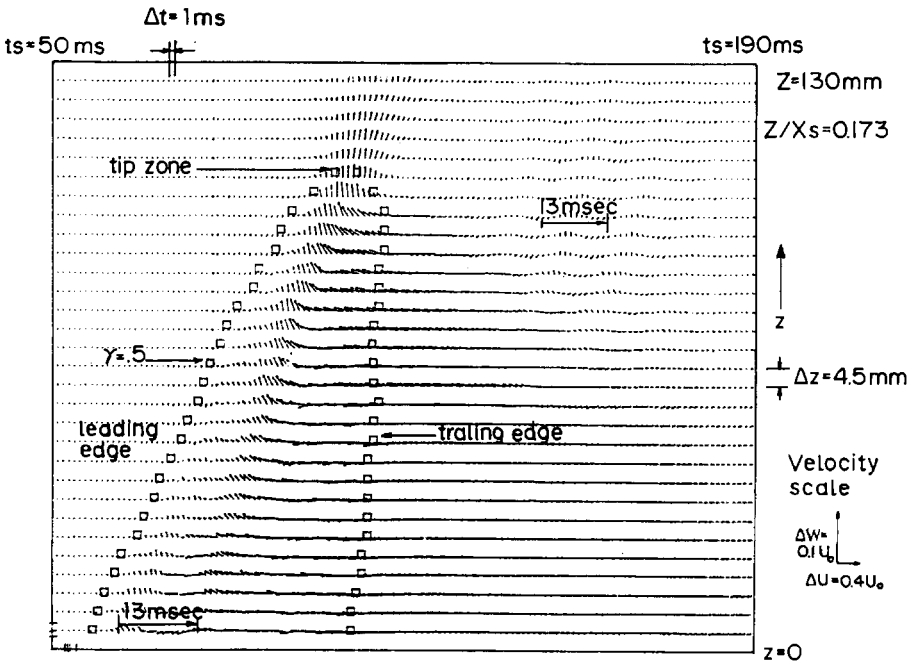

Fig. 10. Vector diagrams of the perturbation velocities in the Z-t plane across the entire spot, $X_s = 75$ cm, $Y/\delta^* = 1$.

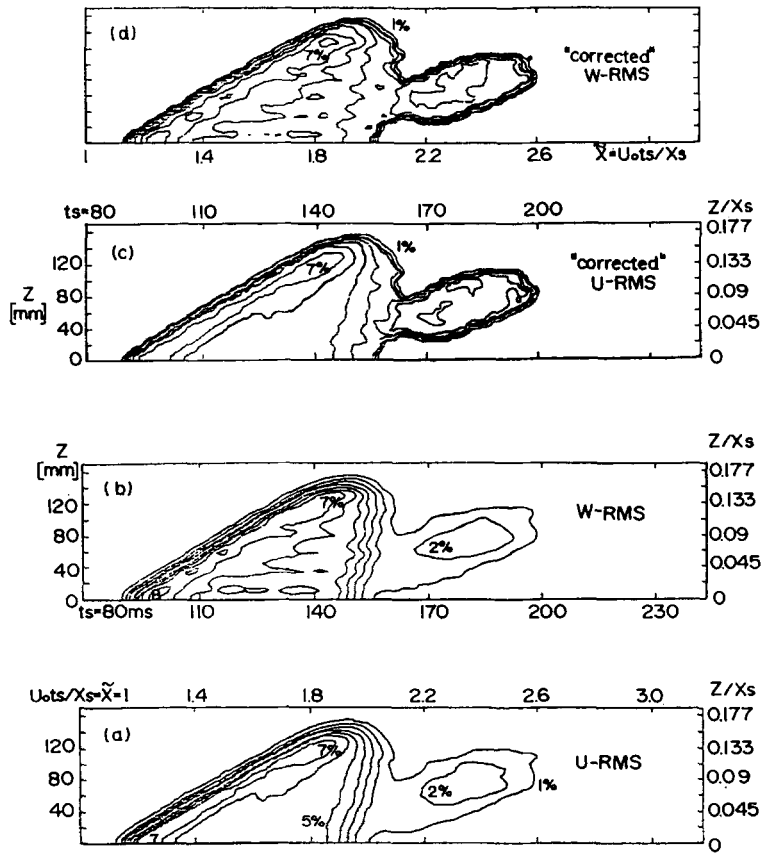

Fig. 11. Turbulent intensities in the spot at $X_s = 75$ cm and $Y/\delta^* = 1$. (a) rms distribution of the streamwise component; (b) rms distribution of the spanwise component; (c) rms distribution of the streamwise component corrected for intermittency; (d) rms distribution of the spanwise component corrected for intermittency.

interfaces but the character of the turbulent intensity distribution does not change by this 'correction' (see the 'corrected' RMS plot shown in Fig. 11c and 11d). Since high turbulence intensities are generally observed following transition, these contours may serve as an additional evidence that the leading interface of the spot destabilizes the laminar boundary layer beneath the 'overhang'.

Concluding remarks

Visual observations of turbulent spots [8–10] reveal that the spot contains a large number of eddies. In fact, provided the Reynolds number is sufficiently high, the structure apparent in the interior of the spot is indistinguishable from the structure of the turbulent boundary layer [8]. Filtered velocity records capturing the entire cross section of a single spot [7] on the plane of symmetry reveal the large number of eddies it contains. Detailed measurements in the 'nascent' spot at low Re landed themselves to a reconstruction of the velocity perturbation associated with the most probable event [11], however the details were lost at higher Re and larger streamwise distances from the origin. It was hoped that the rake of 'V' shaped probes described earlier will provide the needed information and will have a

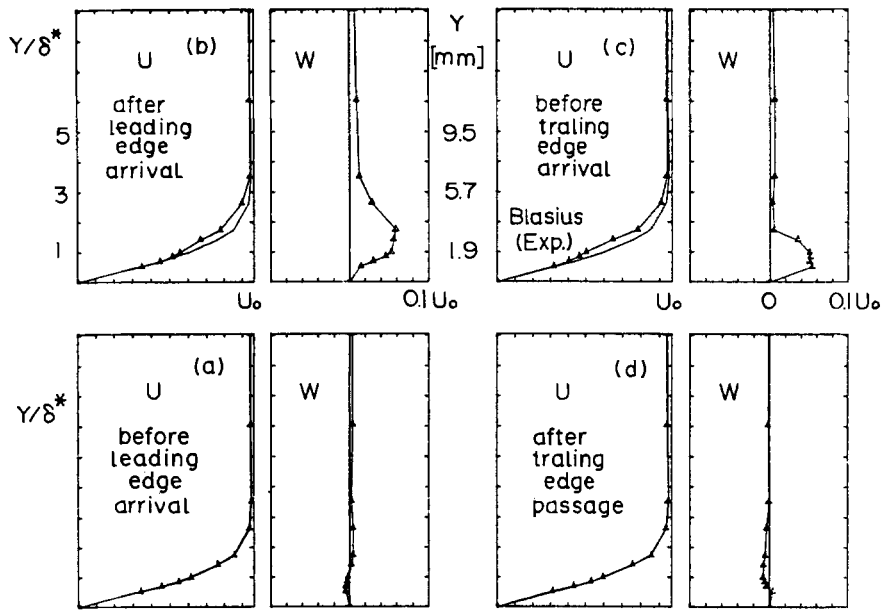

Fig. 12. Instantaneous streamwise and spanwise velocity profiles near the turbulent interfaces of the spot measured at $Z/X_s = 0.149$.

sufficiently good spatial resolution to reveal the substructure near the tip of the spot. Although this hope did not materialize, the data revealed the significance of the cross-flow component which monotonically increased toward the tip of the spot. It appears that much of the entrained fluid near the plane of symmetry and mid-span of the spot is ejected in the spanwise direction outward. Velocity profiles in the streamwise and spanwise directions near the interfaces of the spot at its tip are plotted in Fig. 12. A cross flow component which is non-existent on the laminar flow side of the leading interface is very strong on the turbulent side of it (Fig. 12b and 12c). The streamwise component of the velocity profile is also distorted between $1 < Y/\delta^* < 3$ and possesses an inflection point in that region. Both components of this perturbation velocity are very unstable and may contribute to a rapid breakdown to turbulence. Improved stability analysis of the flow can now be made. Furthermore, novel methods of data analysis like the wavelet technique may avoid the loss of information associated with conventional statistical methods. The current experiment should be supplemented by either Direct Numerical Simulation (DNS) or Large Eddy Simulation (LES) which will include the possible feedback effect between the spot, the wave packets and the 'calmed region'. These effects were not considered by Spalart [12] because of the limited resolution of his calculations.

References

1. I. Wygnanski, J.H. Haritonidis and R.E. Kaplan, On a Tollmien–Schlichting wave packet produced by a turbulent spot. *J. Fluid Mech.* 92 (1979) 505–528.
2. A. Glezer, Y. Katz and I. Wygnanski, On the breakdown of the wave packet trailing a turbulent spot in a laminar boundary layer. *J. Fluid Mech.* 198 (1989) 1–26.
3. Y. Katz, A. Seifert and I. Wygnanski, On the evolution of a turbulent spot in a laminar boundary layer in favorable pressure gradient. *J. Fluid Mech.* 221 (1990) 1–22.

4. I. Wygnanski, M. Sokolov and D. Friedman, On a turbulent spot in a laminar boundary layer. *J. Fluid Mech.* 78 (1976) 785–819.
5. G.B. Schubauer and P.S. Klebanoff, Contributions to the mechanics of boundary layer transition. NACA Report number 1289 (1956).
6. M. Zilberman, I. Wygnanski and R.E. Kaplan, Transitional boundary layer spot in a fully turbulent environment. *Physics of Fluids Supplement* 20 (1977) S258–271.
7. I. Wygnanski, M. Zilberman and J.H. Haritonidis, On the spreading of a turbulent spot in the absence of pressure gradient. *J. Fluid Mech.* 123 (1982) 69–90.
8. B. Cantwell, D. Coles and P. Dimotakis, Structure and entrainment in the plane of symmetry of a turbulent spot. *J. Fluid Mech.* 87 (1978) 641–672.
9. M. Gad-El-Hak, R.F. Blackwelder and J.J. Riley, On the growth of turbulent regions in laminar boundary layers. *J. Fluid Mech.* 110 (1982) 73–96.
10. T. Matsui, Visualization of turbulent spots in the boundary layer along a flat plate in water flow. In: R. Eppler and H. Fasel (eds), *Laminar-turbulent Transition*. Springer Verlag Publishers (1980) pp. 288–296.
11. I. Wygnanski, On turbulent spots. In: G.K. Patterson and J.L. Zakin (eds), *Proceedings of the 7th Biennial Symposium on Turbulence, Rolla, Missouri* (1983) pp. 390–400.